Solid Earth Discuss., 7, 3735–3771, 2015
www.solid-earth-discuss.net/7/3735/2015/
doi:10.5194/sed-7-3735-2015
© Author(s) 2015. CC Attribution 3.0 License.

Solid Earth Discussions
Open Access
EGU

This discussion paper is/has been under review for the journal Solid Earth (SE).
Please refer to the corresponding final paper in SE if available.

Modeling the contributing factors of desertification and evaluating their relationships to soil degradation process through Geomatic techniques

P. Shoba and S. S. Ramakrishnan

Institute of Remote Sensing, Anna University, Chennai, India

Received: 19 November 2015 – Accepted: 19 November 2015 – Published: 9 December 2015

Correspondence to: P. Shoba (shoba84.geog@gmail.com)

Published by Copernicus Publications on behalf of the European Geosciences Union.

Abstract

Desertification is a prolonged stage of land degradation which converts the productive ecosystem to fragile by three crucial events namely evapotranspiration, rainfall and negative human intrusion. The present study concentrates on identifying the causative factors of desertification namely temperature, wind, rainfall and human pressure, distinguishing the desertified land from degraded land and assessing the way from which the soil degradation process gets accelerated by those factors by employing the datasets such as long term (2001–2011) and short term (2012–2015) Meteorological data and Landsat ETM+ and OLI satellite imageries of crop growing period (June–October) into geostatistical methods and newly proposed remote sensing models which yielded good accuracy with in situ observations (R^2 = 0.8). In temperature induced desertified region, the rate of increment of the saline affected region was magnified significantly from 16 to 74 % (2001–2015) due to the presence of native fluoride concentration and extreme temperature event over a period of time. The long term exaggeration of soil moisture stress (19 to 90 %) has been notified in the areas that were susceptible to wind induced desertification, due to high evaporation rate invoked by extreme wind event for a substantial period. Similarly rainfall induced desertified regions have also been experiencing high soil moisture stress (4 to 70 %) because of the insufficient reception of rainfall. High human made soil salinity (36 %), human occupancy (16 %), followed by moisture stress (7 %) are observed in the human affected region because of growing population and improper land management of the already fragile land.

1 Introduction

Desertification is defined as “Degradation of the soil, landscape and bio-productive terrestrial system, in arid, semi-arid and sub-humid areas resulting from several factors including climate change and human activities” (UNCCD, 1994). Desertification is generally perceived as slow hazard in semi-arid region, initially provoked by climatic factors

SED
7, 3735–3771, 2015

(persistent droughts due to insufficient rainfall event, extreme intolerable temperature events, severe wind etc.) and gets accelerated when combined with human actions (population pressure, intensive land use, improper land management etc.) and indigenous geological environmental state prevailing on a longer time frame (Lin and Tang, 2002), which produces an adverse effect to people and the ecological system. Among many events which affect earth's environment and ecosystem, drought is often having direct association with desertification (Shewale and Shravan kumar, 2005). Drought, a period of unusually dry weather with poor land management, can cause loss of vegetation, which in turn leads to desertification (Sharmia Sultana, 2008). Desertification is the end stage of land degradation process (Hill et al., 2005) which ultimately affects the economical and biological productivity of the land (Izzo et al., 2013) by degrading soil fertility completely.

Though desertification inducing factors have produced immense negative effect on many environmental components, soil is a prime component that gets deteriorated by the process. Once the physical, chemical and biological properties of the soils started degrading, the natural regeneration is not possible in an expected human time frame (UNCCD, 2012). Its replenishment rate is very slow on human time scale, hence termed as nonrenewable resource. Roxo et al. (2001) have defined desertification in the perception of soil degradation through the continuous loss of soil fertility by damage of structure and composition of the soil which ultimately affects the sustainable agricultural production. Since desertification impact is directly on the soil, it becomes necessary to identify the prime causative factors which accelerate the desertification and evaluate the soil degradation process stimulated by those factors in order to protect the precious resource before it loses its capacity entirely.

Remote sensing technology is successfully applied to the process of monitoring desert expansion and the assessment of factors that cause desertification (Hanan et al., 1991). The land degradation of arid and semi-arid zones often called as desertification when it is irreversible in form and the factor of this phenomena either climate or human has been much debated since the mid-1970s (Rasmussen et al., 2001). Climate

SED
7, 3735–3771, 2015

fluctuations and human activities together induces desertification in semi-arid region, their individual impacts should be assessed in detail in order to resolve the ambiguity over which is the primary cause (Runnstrom, 2003 and Wang et al., 2006). Besides, rainfall, temperature and wind are also important climatic factors which can accelerate the desertification through the process called evapotranspiration. The evapotranspiration (ET) is a combination of evaporation of water from soil surfaces and vegetal transpiration. ET is key element to assess water resource scarcity in vegetation and soil as well, in semi-arid and arid regions (Chen and Rao, 2008). The production of rain fed crops could be directly related to the rate of evapotranspiration (Geeson et al., 2002). ET has a strong correlation with Enhanced vegetation Index (Nagler et al., 2007) which makes the sense that ET and vegetal degradation effects are dependent to each other.

Though many models have emerged for calculating evapotranspiration since 1948, FAO Penman–Monteith has been considered to be the best method till today for Indian condition (Bapuji et al., 2012). Though the evapotranspiration highly depends upon all weather parameters such as rainfall, temperature, solar radiation, humidity and wind speed, it is majorly influenced only by temperature and wind speed (energy with respect to air movement) (Dodds et al., 2005). There is not much report emphasized on identifying the accelerating factor of desertification by considering evapotranspiration along with NDVI and rainfall so far. This is the first time the spatial correlation models have been developed with the combination of evapotranspiration, NDVI and rainfall in order to predict the temperature, wind, rainfall and human affected zones of desertification. Furthermore the present study identifies and extracts the completely desertified area from the degraded area with the help of recent short term negative vegetation trend which was lacking in the previous studies. The reason behind the incorporation of recent short term vegetal trend in the present study is, “in semi-arid regions the ecosystem retains its consistency and ability to respond to the recurrence of the rainy season” (Kassas, 1977). If the degraded land is not responding to the adequate rain, it is termed as desertification.

SED
7, 3735–3771, 2015

After the identification and evaluation of the causative factors, the study also focuses on the crucial soil degradation components that get accelerated through those factors. The study region has naturally inherited high fluoride content from the ground water. Positive correlation between Fluoride and pH indicated that alkaline condition improved solubility of Fluoride (Adhikary et al., 2014). The ground water salinity has been carried to the sub surface and some surface level of the soil through capillary action and during the extreme temperature event the saline water is evaporated and salt remains accumulated. Hence, area that is affected by desertification due to high temperature factor should have definitely experienced the soil salinity because of temperature induced ET and native fluoride content; similarly the desertified area due to wind speed would have experienced soil moisture stress at surface level and rainfall factor would have experienced soil moisture stress at surface and sub-surface level (root zone).

Hence the testable directional hypothesis was framed in order to prove the above said theoretical anticipation. Directional hypothesis is usually framed in such a way to predict the specific relationship between the components and direction of that relationship. After the execution of testable hypothesis, the Diagonal Soil Moisture Stress Index (DSMSI) has been proposed in the current study to extract the moisture stress areas from the imagery with reasonable accuracy. Similarly Diagonal Soil Salinity Index (DSSI) was created to identify the saline affected soils of study region. Tasseled cap transformation (TCT) parameters such as Brightness Index (BI) and Wetness Index (WI) (Guo et al., 2011) have been used for evaluating the theoretical dependability of the models.

The prime objective of the study is (i) to identify and differentiate different zones of degradation and desertification with respect to temperature, wind, rainfall and anthropogenic factors using geo-statistical model. (ii) To frame the hypothesis in such a way to prove theoretical anticipation of what soil degradation process can be expected from each zone of desertification. (iii) To quantify and assess the possible soil degradation processes namely soil moisture stress and salinity at surface and sub-surface level

SED
7, 3735–3771, 2015

through remote sensing models and techniques. (iv) To validate the work to assure the reliability of the geo-statistical and remote sensing models through in situ observations.

2 Materials and methods

2.1 Study region and prevailing problems

Dharmapuri is located in the North–Western climate zone of Tamil Nadu, India. It lies between 11°47′ and 12°33′ degrees of Northern latitude and 77°28′ and 76°45′ degrees of Eastern longitude. The annual potential evapotranspiration rate in this region is 1727 mm compared to the annual precipitation of 825 mm. It is a dry and semi-arid production system (Fig. 1). The study region has been facing maximum temperature of about 37 °C in the month of April–May. Rhodustalfs, Ustropepts and Rhodic Paleustalfs (Soil Survey Staff, 1975) are the dominate soil taxa found in the site with high presence of loam and clay which stimulates the capillary action while experiencing high temperature. Sorghum, finger millet and little millet are the major field crops of Dharmapuri District, whose spatial distribution is about 34 000 ha, which supports 70 % of the population. The Socio-economic condition of the region is very poor due to poor rainfall and frequent monsoon failure and thus leading to drought in many parts of the region (Anbazhagan et al., 2013). The drought is the visible evident of a degrading ecosystem in which land is a main component (Budihal et al., 2005).

The District is also facing strong salinization, affecting 2 % of land. About 1 % of land is affected by water logging and it is proved with the presence of hard pans (Fig. 5e). The entire "territory" is having water scarcity and out of five "tehsils", four are over exploited (Central Ground water Board Report, 2009). Presence of Fluoride is more than the permissible limit (above 1.5 mg L^{-1}) in the study region (Sendesh et al., 2011; Ramesh and Vennila, 2012). Positive correlation between F and pH indicated that alkaline condition improved solubility of Fluoride (Adhikary et al., 2014a). So ground water in aquifers in general, is slightly alkaline in nature (Central Ground water Board Report,

SED
7, 3735–3771, 2015

2009a). The erratic climatic events, socio-economic developments and unsustainable agricultural practices in the past decades, exert strong pressure on fertile land of the study region.

2.2 Satellite data

Since MODIS and NOAA AVHRR satellites have high temporal resolution, they have been adopted for long term change detection, land degradation and desertification analysis so far by various researchers across the world. But the limiting factor which hinders the applicability to employ those imageries in the sub-regional level assessment is low spatial resolution. Therefore, moderate spatial resolution with long term temporally available imageries are required to assess the phenomena at sub-regional level. Landsat satellite imageries have the longest spatial record for land observation (Williams et al., 2006). So, the present study is carried out using ETM+ (Enhanced Thematic Mapper) and OLI (Operational land Imager) Imageries on board Landsat 7 and 8 Mission from 2000–2015. Totally eight bands starting from 30 m Blue (0.441–0.514 µm) to 15 m Pan (0.515–0.896 µm) of electromagnetic spectrum are utilized in the ETM+ mission where as the arrangements and the inclusions of bands are little bit modified in OLI mission. Band 1 is a deep blue band for coastal/aerosol studies and band 11 is a shortwave infrared band for cirrus detection in OLI mission.

The two satellites are in a sun-synchronous, near-polar orbit at 705 km altitude and have the moderate spatial resolution of 30 m for multispectral bands. ETM+ data of path no 143 path and row no 52 were collected from 2001–2012 and OLI imageries were collected from 2013–2015 from Glovis online free resource center. Bands are stacked and Subset operation has been performed in order to clip the imagery with respect to study area. From 2004 to 2012 the Landsat 7 mission has acquired the data with Scan Line Corrector (SLC) off mode. SLC images are collected for the corresponding years, spatially corrected using focal analysis and spectrally equalized using histogram equalization method to make the data ready for further geo-spatial analysis as illustrated below.

SED
7, 3735–3771, 2015

2.3 Meteorological data and desertification phase identification

Daily meteorological datasets such as rainfall, minimum temperature, maximum temperature, wind speed, solar radiation and relative humidity from 2001–2015 have been collected from Centre for climate change and adaptation research, Anna university, India. Dharmapuri is one of the districts of Tamil Nadu, India which gets benefited by Kharif season or South–West monsoon rain (June–October). So the crop growth is considerably high from June to October. There are 6 meteorological stations, distributed in and around the study region. Plotted points are interpolated using IDW (Inverse distance weighted) method with same resolution (30 m cell size) of Landsat data. The minimum temperature, maximum temperature, wind speed, solar radiation, relative humidity and rainfall raster of different months of growing season are then averaged to obtain the mean values of growing season of each year.

Land degradation to desertification phase identification plays a vital role before entering into an assessment of desertification. The phase can be initially identified through rainfall and temperature distribution. The land degradation period has to be identified in order to recognize the period when the desertification invokes. From 2006 to 2011 there was a significant decline in rainfall and increment in temperature followed by immediate high rainfall occurred in 2012 (Fig. 2). So the land degradation should have occurred between 2006–2011 time frame. If the land degradation is not responding to the immediate high rainfall that occurred in 2012 and prolonged to 2015, then it is termed as desertification else, it is just land degradation.

2.4 NDVI topographical normalization

Before estimating the NDVI (Normalized differential Vegetation Index), the bands of the imageries have to be topographically normalized in order to eliminate the effects from shadowed region on NDVI imagery. Bands 3 and 4 of ETM+ and OLI are topographically normalized using modified cosine correction (Meyer et al., 1993) to eliminate the illumination variation which hampers the ability to discriminate ground fea-

SED
7, 3735–3771, 2015

tures, as the same features will have different spectral responses among shadowed and non-shadowed region. It is very important to eliminate the topographical effects in the present study as the correlation analysis is highly affected by the shadow region. For instance, the water body in the NDVI and rainfall has no correlation over a period of time, thus the result of the correlation analysis should be zero in those places. Some locations of the eastern part of the region are occupied by shadow because of the slight elevation and dense vegetation. Due to the presence of dense vegetation and occurrences of high rainfall, the area has to be shown as highly correlated. But the shadow region is considered as a water body by the model because of the spectral coincidence of shadow region and water body and the resultant correlation is zero (no correlation). Hence some portion of high dense vegetation area has high possibility to be wrongly estimated as no correlation if the topographical effects are not eliminated. After applying the normalization to the bands, the eastern and western parts (hilly region) of the NDVI has been well enhanced.

2.5 Reference evapotranspiration (ET_{ref})

Understanding the influence of ET on the land degradation and desertification process is important when dealing with semi-arid environment. High ET rate adversely affects the biodiversity of dry land eco-system and accelerates the desertification process especially by temperature and wind event. The Penman–Monteith evapotranspiration model is developed in such a way to suit meteorological data and significantly estimates the rate of evapotranspiration from a reference grass crop (Dodds et al., 2005a). FAO Penman–Monteith method is conceived as the best method through which the ET_{ref} can be explicitly determined and consistent values are obtained for all regions and climates (Allen et al., 1998).

Penman–Monteith equation has been spatially modeled in the ArcMap environment in order to extract the seasonal rate of change of ET_{ref} in the study region from 2001–2011. The spatial model is generated with the frame work of original Penman–Monteith equation (Eq. 1). The collected monthly Meteorological data such as minimum temper-

SED
7, 3735–3771, 2015

ature, maximum temperature, wind speed, solar radiation and relative humidity of crop growing period (June–October), latitude, Julian day and Elevation from 2001–2011 are given as an input for the spatial model in order to extract the spatial reference evapotranspiration.

$$ET_{ref} = \left[\frac{0.408\Delta\,(R_n - G) + \gamma\left[\frac{900}{T+273}\right]\mu_2(VPD)}{\Delta + \gamma\,(1 + 0.34\mu_2)}\right] \quad (1)$$

where
ET_{ref} = daily reference ET [mm d^{-1}],
T = air temperature at 2 m high [°C],
VPD = vapor pressure deficit [kPa],
μ_2 = wind speed at 2 m high [m s^{-1}],
R_n = net radiation at the crop surface [MJ m^{-2} d^{-1}],
Δ = slope vapour pressure curve [kPa °C^{-1}],
γ = psychometric constant [kPa °C^{-1}] and,
G = soil heat flux density [MJ m^{-2} d^{-1}].

2.6 Spatial regression model

A strong linear trend was identified between NDVI and 3 months cumulative rainfall (Nicholson et al., 1990). Since the rainfall and NDVI follows linear trend, spatial linear regression model is formulated by taking rainfall as an independent variable and NDVI as a regressed parameter. The regression analysis has been performed for each year from 2001 to 2011 after computing slope and intercept for each pixel, in order to yield the result of the long term NDVI that should have been present in the study region with respect to rainfall hence called $NDVI_{predicted}$.

SED
7, 3735–3771, 2015

2.7 Spatial correlation coefficient model

In order to identify the negatively correlated area where the vegetation stress is dependent on high evapotranspiration, the spatial correlation coefficient analyses is done for long term mean reference evapotranspiration (ET_{ref}) and mean predicted NDVI ($NDVI_{predicted}$) (Fig. 6b). Though evapotranspiration depends upon many factors such as temperature, solar radiation, humidity, wind speed, the energy consumed by wind and temperature is higher than the above mentioned factors. Thus, the correlation coefficient analysis is again performed for ET_{ref} – temperature (R^2 = 0.8) and ET_{ref} – wind speed (R^2 = 0.83) in order to extract the temperature and wind affected zones of land degradation and desertification.

The region of positive correlation (ET_{ref} – $NDVI_{predicted}$) is an indication of the condition where the vegetation has been resisted even after experiencing high evapotranspiration due to the reception of adequate rainfall. The Spatial correlation coefficient analysis was again performed between $Rainfall_{mean}$ and $NDVI_{predicted}$ on the positively correlated area of ET_{ref} – $NDVI_{predicted}$ in order to identify the rainfall and human induced desertification.

2.8 $NDVI_{normalized}$ trend analayis

Statistically-significant negative slope in the NDVI time series is an indicator of the degradation (Wessels et al., 2007). The long term vegetation stress can be well identified and monitored by long term NDVI data and thus used for desertification assessment (Kundu and Dutta, 2011). The time trend analysis has been performed for long term NDVI to identify the spatio-temporal gradual and sudden changes in the vegetation condition of the study region over a period of time. Long term (2001–2011) (Fig. 6a) and short term (2012–2015) trend has been estimated spatially for Maximum NDVI.

SED
7, 3735–3771, 2015

2.9 LULC (Land Use and Land Cover mapping) (2001, 2005, 2010 and 2014)

At regional level both supervised and unsupervised classification works good for extracting soil salinity (Naseri, 1998). Supervised classification was performed for Landsat Satellite imageries of 2001, 2005, 2010 and 2014 in order to classify the saline, non-saline soils, wet lands and human structures. Maximum likelihood algorithm has been implemented in the supervised classification. About 50 in situ observations are used as samples for training the system to classify the imagery. The Level 1 land cover types namely Forest region, agricultural land, wet land, built-up, barren land and water body were identified in the study region with the help of ground knowledge. The overall accuracy of the work was verified through confusion matrix and the attained accuracy of the classification was 91 %. It was observed that the saline affected regions and human occupancy rate were increased at an accelerated rate from 2001–2014.

2.10 Diagonal Soil Moisture Stress Index (DSMSI)

Few authors like Moren et al. (1994), Sandholt et al. (2002), Shafian and Mass (2015) have proved the potential of triangle and trapezoidal model on Temperature – Vegetation scatter plot in the extraction of soil moisture with adequate accuracy level (R^2 = 0.703). The study region should have been facing soil moisture stress due to low rainfall distribution, high wind speed and extreme temperature event during the crop growing period from 2006 to 2011. Based on the pattern of the scatter plot of NDVI and TIR (Thermal IR) band (Fig. 3a), we proposed the new model called DSMSI with the association of wind speed to increase the accuracy and reliability of the soil moisture stress.

The distribution pattern of NDVI with respect to TIR band follows a shape of inclined rectangle. From the rectangle we found two wet edges and two dry edges based on their position on the scatter plot. Edge 1 and 2 are wet edges and 3 and 4 are dry edges. The diagonal line is formed from the edge 1 to edge 4 as edge 1 is extremely wet compared to edge 2 and edge 4 is extremely dry compared to edge 3. The wet-

SED
7, 3735–3771, 2015

ness or moisture decreases with increasing diagonal distance from extreme wet edge 1. The diagonal distance has an inverse relationship with NDVI and direct correlation with wind speed. As shown in Fig. 3b the perpendicular line (a) erected from extreme wet (edge 1) to the line of edges 2–4. The pixels located at the left side of the line are healthy vegetation because of the high NDVI value and low temperature. Similarly, perpendicular line (b) is again erected from extreme dry (edge 4) to the line of edges 1–3. The pixels located at the right side of the line are extremely dry, thus termed as saline affected soils. The pixels located in between the line a and b, depict the level of soil moisture stress. Hence, the scatter zone has been divided into three parts namely healthy vegetation, soil moisture stress and saline zone. So, there is strong convergence existing between soil moisture stress and salinity at the extreme diagonal zone. To reduce the misinterpretation of saline zone as an extreme soil moisture stress zone and to increase the veracity of the DSMSI model in terms of soil moisture stress, the extreme portions of the resultant values are avoided and the most influential parameter of moisture stress, wind speed was included in the equation.

Like temperature, the wind speed also influences the moisture content in the surface soil, which is not considered in the previous studies. Since the diagonal distance or moisture stress is inversely proportional to NDVI and directly proportional to wind speed, the model has been framed as shown in the Eq. (2). TIR band and average wind speed of the growing period were normalized before feeding it in to the equation. Soil moisture stress maps of four years (2001, 2005, 2010 and 2014) have been mapped using DSMSI model (Eq. 2). DSMSI model is a function of NDVI, TIR and Wind speed.

$$\mathrm{DSMSI} = \left[\left(\frac{\mathrm{TIR}_i + (\mathrm{ndvi}_{\max} - \mathrm{ndvi}_i)\sqrt{2}}{(1 + \mathrm{ndvi}_i)} \times 0.5\right) + (\mathrm{ws}_{i\text{-norm}} \times 0.5)\right] \times 100 \quad (2)$$

where
DSMSI = Diagonal soil moisture stress index (%),
TIR_i = ith pixel of normalized TIR band,

SED
7, 3735–3771, 2015

$ndvi_{max}$ = maximum value of NDVI,
$ndvi_i$ = ith pixel of NDVI and,
$ws_{i\text{-norm}}$ = ith pixel of normalized wind speed ($m\,s^{-1}$).

The values of the model vary from 0 to 100 in which 0 indicates sufficient moisture content in the soil, 100 indicates the extreme dryness and intermediate values illustrates the moisture stress severity levels. DSMSI model has been regressed with TCW_{ETM+} (Tasseled cap wetness index) (Guo et al., 2011a) in order to assess the theoretical reliability of the result initially. And it yielded a best fit with TCW (R^2 = 0.782) (Fig. 3c).

2.11 Extraction of saline affected soil

Saline soils are very difficult to identify because of its dynamic nature. Dry areas are naturally prone to soil salinization due to occurrence of low rainfall and high evapotranspiration which limits the leaching of salts and this effect is expected to be magnified when its combined with human's negative intrusion like over fertilization on farming land (Metternicht and Zinck, 2009). Allbed et al. (2014) found that the Salinity Index (SI) and red band (band 3) have significant correlation with Electrical conductivity (EC). Though many research have been carried out in the field of soil salinity identification so far through various models like SI, Normalized Differential Salinity Index (NDSI) etc., still an extraction of soil salinity needs more accuracy because of the confusion created from the same spectral signature values of settlement roofs and saline affected zones in the study region. So additional independent variables have to be involved in the analysis in order to reduce the places of uncertainty. Abdul-Qadir and Benni (2010) found that MIR band has shown high correlation between SI and NDSI. Since the diagonal distance of scatter plot (Fig. 2a) had the similar relationship with soil salinity as the salinity increases with increasing diagonal distance, the same model was used in association with MID-IR band for deriving a new model named as Diagonal Soil Salinity Index (DSSI) which has increased the accuracy of extracting surface soil salinity at the

SED
7, 3735–3771, 2015

extreme ranges. Inclusion of MID-IR band in the model has significantly reduced the effect of soil moisture and building roofs on extracting salinity.

Spectral plot of the study region shows that the saline affected region can be separated from the settlements from 0.7–1 (after normalization) range in the MID-IR region. Low organic matter exhibits higher reflectance in the MID-IR region rather than the settlements. The diagonal distance of the right angle triangle, observed from the extreme corner of the scatter plot of MID-IR and NDVI, was considered as a saline line where the salinity increases with increasing distance from an apex point (NDVI = 0.5 and MID-IR = 0.7). The negative values of the model were eliminated in the analysis, as the saline affected regions maintain the range above 0.7 in MID-IR region and below 0.5 in NDVI.

$$\mathrm{DSSI} = \left[\frac{(\mathrm{TIR}_i + (\mathrm{ndvi}_{\max} - \mathrm{ndvi}_i))}{((\mathrm{MIR}_i - 0.7) + (0.5 - \mathrm{ndvi}_i))}\right] \quad (3)$$

Since the study region is expected to experience soil salinity because of the fluoride origin and extreme temperature event, surface level soil salinity was derived for the years 2001, 2005, 2010 and 2014 using Diagonal soil salinity Index model (Eq. 3) as it yielded a best fit with TCB (Tasseled cap Brightness index) (R^2 = 0.86) (Fig. 4a).

2.12 Testable directional hypothesis

Directional hypothesis was framed in such a way to prove the expected direction of relationship between temperature – salinization, wind – soil moisture stress, and rainfall – moisture stress at 0.05 % confidence level. Based on the hypothesis the rejection area i.e., the area of high correlation existence between the variables, has been extracted for each case and shown in Table 1. For temperature–salinity combination, the computed value of t statistic (t = 4.645) is higher than tabulated one (t = 3.482) at 0.05 level of confidence and this statement confirms the adequacy of the positive correlation between salinity and temperature. As anticipated, the salinity is a predominant degradation process in temperature affected zone. Likewise other combinations have also

SED
7, 3735–3771, 2015

proven its adequacy for higher correlation. The rainfall–moisture stress combination t values (−3.248) has fallen in the negative region of histogram as the moisture stress is negatively correlated with rainfall.

2.13 In situ observations

In situ measurements are taken (Fig. 5b) for the chemical characteristics of the soil such as soil salinity, EC (Electrical conductivity), pH, temperature and soil moisture at 100 locations in and around the study region using EI Deep Vision water and soil analysis equipment (Model 161). Questionnaire survey has also been conducted with the inhabitants of the study region along with the field measurements in order to familiarize with the socio-economic condition of the people, their land management practices and their awareness towards land degradation process. Soil samples are collected at both surface and sub-surface level (Fig. 5f) and dissolved with ground water of that region in order to facilitate the process of measuring chemical parameters as listed in Table 2.

The sub-surface salinity or EC is significantly higher (mean 6.5 $mS\,cm^{-1}$) than the surface salinity (mean 4.2 $mS\,cm^{-1}$) in the temperature affected zone because of the fluoride origin and the extreme temperature prevalence. Conversely the surface EC values are higher than the sub-surface in the human affected region. From the questionnaire survey conducted with the local farmers (Fig. 5a), the reason was identified to be long term application of fertilizers for more than 2 decades which raises the salinity in the soil more than the fluoride does. In the human affected regions, extreme surface salinity is observed in few low lying areas (Fig. 5c), because of the leaching of fertilizers from surrounding elevated areas. The distribution of salinity is discrete in the human affected regions whereas it follows a continuous pattern in the temperature and wind affected region (climate influenced region). Oleander (*Nerium Oleander L.)* is the only shrub planted in this affected region so as to withstand salinity. With this information, we discriminated salinity even under the vegetation while classifying Landsat imagery.

Due to the migration of native people for their economic needs, the land was left abandoned for years together which kept increasing the salinity with the absence of

SED
7, 3735–3771, 2015

land management practices. In addition to that, farmers keep spending money for the land reclamation more than what they can get in return from the land without knowing the actual condition/productivity of the land. In the dry areas, drip irrigation is practiced to achieve the needs of the growing population at the time of insufficient rainfall. Human occupancy such as real estate, urbanization has started intruding the agricultural land which substantially affects the productive eco-system. As hypothesized, the soil moisture stress (Fig. 5d) in the wind induced desertified region (18 052 ha) and rainfall induced desertified region (5146 ha) is comparatively higher than the temperature (4015 ha) and human (1042 ha) induced region.

3 Results and discussion

3.1 Temperature and wind induced degradation using evapotranspiration rate

Form the spatial correlation analysis between long term mean reference evapotranspiration and mean predicted NDVI (Fig. 6b), we found that 61 % (252 568.08 ha) of land is negatively correlated, 34 % (139 357.98 ha) of land is positively correlated and 5 % (21 842.64 ha) is experiencing no correlation because of the stable NDVI over a period of time. The negatively correlated area is the direct illustration of NDVI reduction due to the high evapotranspiration rate over a period. The land degradation due to evapotranspiration is identified if the negative $NDVI_{observed}$ trend (Fig. 6a) is observed in the negatively correlated area. Among 44 982 ha of evapotranspiration affected area, 55 % (24 869 ha) of land parcel was affected by temperature and 45 % (20 113 ha) were affected by wind. Hence temperature and wind induced degraded area has been identified from the analysis. Wind affected zones are nothing but the degraded land due to high evapotranspiration rate, which highly depends on wind speed rather than temperature. Similarly temperature affected zones are the degraded land due to high evapotranspiration rate, which is highly induced by temperature rather than wind speed.

SED
7, 3735–3771, 2015

3.2 Rainfall and human induced degradation

Spatial correlation coefficient analysis was performed for rainfall and $NDVI_{pred}$ of positively correlated area of ET_{ref} and $NDVI_{pred}$. This is the region where the vegetation has maintained its consistency even after experiencing high evapotranspiration by temperature and wind over a period of time. So if the degradation is suspected to occur in this region, it's mainly due to rainfall or human factors. Rainfall induced degradation was identified if the negative $NDVI_{observed}$ trend is observed in the positively correlated area. Similarly, human induced degradation was identified if the negative $NDVI_{observed}$ trend is observed in the negatively correlated area. Among 139 357.98 ha, 25 % (34 779.96 ha) are affected by insufficient rainfall and 30 % (42 184.26 ha) are affected by human intrusion. Figure 6c depicts the degraded zones with respect to temperature, wind, rainfall and human factors.

3.3 Land degradation to desertification

As discussed earlier, if the degraded land is not responding well to the sufficient rainfall, then it is termed as desertification. Desertified land area is identified by considering short term NDVI (2012–2015) trend when the rainfall rate is sufficient enough for the plant growth. Desertified area has been extracted where the degraded land is still facing negative short term NDVI trend. About 70 % (121 179.15 ha) of the degraded land would have been wrongly identified as desertified land if the short term NDVI trend is not included in the analysis. The research found that 5 % of the total area (439 189.71 ha) is in desertified state. Figure 6d illustrates the four zones of desertification due to temperature, wind, rainfall and human events.

SED
7, 3735–3771, 2015

3.4 Soil degradation process induced by temperature, wind, rainfall and human intrusion

Soil degradation process invoked by the four crucial factors are recognized and validated in the present study as soil is the predominant component which gets deteriorated by the process. Red gravelly clay soil is predominately found in the temperature affected region. Fine pores soil like clay has greater ability to retain the water through capillary action. So, the soil of the temperature affected region has been naturally inherited high fluoride content from the ground water through capillary action. During the extreme temperature, the saline water at sub surface and some surface level of the soil has been evaporated and salt remains accumulated as cited earlier. Higher fluoride content and extreme pH has high positive correlation and thus enables the water and soil to experience salinity (Adhikary et al., 2014b).

As hypothesized, the temperature induced desertified area should have been strongly affected by salinity. Higher salinity hinders the vegetation growth and thus supports the water erosion and saline leaching process during the occurrence of extreme rain soon after the long term insufficient rainfall which happened in 2012. Hence the anticipation was carried in the temperature zone where soil salinity should have been accelerated due to native fluoride concentration on ground water and high evapotranspiration induced by temperature over a period of time. Surface level soil salinity was estimated for 2001, 2005, 2010 and 2015 using DSSI model as it yielded a best fit with ground truth measurements (R^2 = 0.803) (Fig. 3b). Area of soil salinity has been significantly increased from 16 to 74 % in the temperature affected regions than the area of soil moisture stress (4 to 23 %) from 2001 to 2015. Though the soil moisture stress is being steadily increased due to high temperature prevalence, the increment rate of surface salinity is exceeding at an unexpected rate over a period of time (Fig. 7a). Particularly from 2005–2010 (degradation phase) the area of increment of salinity was about 26 % from which 20 % of the saline track persisted same in 2010–2015 time frame (desertification phase), which indicates that only 6 % of land parcel has got re-

SED
7, 3735–3771, 2015

newed in the temperature induced desertified zone. Hence the initial anticipation has proved that the temperature affected zone should have emphatically experienced high amount of soil salinity than other soil degradation factors.

Based on the directional hypothesis, the wind affected region is expected to experience soil moisture stress at the surface level. So, the further component called surface soil moisture stress for 2001, 2005, 2010 and 2015 were extracted through the DMSMI model and it yielded a best fit with in situ observations (R^2 = 0.804) (Fig. 3d). The area of surface soil moisture stress is increased constantly (19 to 90 %) from 2001 to 2015 in the region where wind is the predominant inducing factor. Soil salinity in those regions are somewhat fluctuating at a lower rate (8 % in 2001, 9 % in 2005, 7 % in 2010 and 6 % in 2015) and that too due to native fluoride content. During the degradation phase from 2006–2011, we found higher rate (63 %) of soil moisture stress has been invoked by the wind (Fig. 7b).

Similarly rainfall induced desertification has also provoked the soil moisture stress at surface and root zone (sub-surface) especially from 2006–2011 time frame and this effect was still in elevated rate from 2012–2015 (Fig. 7c). The low rainfall will decrease the decomposition rate in the soil, thereby reducing the nutrient content in the rainfall affected regions. So, nutrient losses are observed in the rainfall affected zone along with soil moisture stress from in situ observations. Though the moisture stress was obtained at surface level effectively in the rainfall affected region using DSMSI model, we couldn't model the sub-surface moisture stress as we have dealt with optical imagery which does not have surface penetration capacity.

The consequences of the above three declared factors of desertification namely rainfall, wind, temperature are slow and can be suspected and quantified with respect to past, current and future prediction models as it solely depends on climatic variables. But the fourth factor called human activities produce adverse effect on the land in an unexpected and rapid manner and cannot be predicted in advance. According to Vieira et al. (2015) the human activities are the predominant factor for desertification expan-

SED
7, 3735–3771, 2015

sion. The human induced desertified regions were affected by salinity, human occupancy followed by moisture stress (Fig. 7d).

Human made salinity was increased by 9 % in the degradation phase and gets accelerated in desertification phase (14 %). About 5 % of the saline track has been increased in the desertification phase. Dissolved nitrate is the main source for the concentration of fluoride in the ground water. There is no evidence for the geological source of nitrate (Ramesh and Vennila, 2012) in the human induced desertified region. Therefore, it was resultant from human activities. The fact has been well understood from the results obtained from questionnaire survey i.e. the long term application of fertilizers (more than 2 decades) raises the salinity in the ground water and the soil as well. Hence, the substantial increment of salinity in the human affected zone was due to the high application of fertilizers on already fragile land to achieve high production rate, more than its sustainable capacity in order to support the growing population.

Furthermore the human occupancy is significantly increased from 2001 to 2015 particularly in the degradation period (2006–2011). This is due to the increment of population (8 %) from 2001–2011 (Fig. 8) in the human affected region. Population growth of the other regions (temperature affected, rainfall affected and wind affected) has followed decreasing trend from 2001–2011, which is the direct illustration of migration of the inhabitants to urbanized areas due the long term drought conditions existing. About 38 % of decadal growth (2001–2011) of the population was particularly measured in the urban areas of the study region (Census of India, 2011). So, during the aridity stage, human pressure should have been started on the agricultural land in order to support the growing population or attain the financial security as the agricultural practice was not that much feasible in the period. Figure 7d depicts the rate of increment of salinity and urbanization. Soil moisture stress had little effect in the human affected region, which increases only by 1 % during the degradation phase.

The standard deviation of sub-surface EC and Salinity is significantly higher (1.46 and 1.49) than the surface level which shows the values of the salinity are highly fluctuating at the sub-surface level (Table 1) particularly in human affected zone. Hence,

SED
7, 3735–3771, 2015

DSSI model has yielded poor accuracy for sub-surface level (R^2 = 0.5), as the sub-surface salinity is considerably lower than the surface salinity in the human affected region. This is because of the leaching of salts due to the application of excess amount of fertilizers for more than two decades.

4 Conclusions

The proposed study carried four driving forces such as temperature, wind, rainfall and human for the assessment of land degradation and desertification with the aid of appropriate geo-statistical model. This new method evaluates the highly influential soil degradation process on each affected zone, which enables us to weight each soil degradation process based on the influence while quantifying the desertification. More over the appropriate models can be selected to the area based on the suspected soil degradation process for desertification quantification, because we cannot apply soil erosion model to the region which has been affected by salinity over the years. But some of the limitations are there in the present work which has to be carried out in the future research work, (1) Wind affected region would have also been facing strong wind erosion, but only soil moisture stress was studied, (2) Either soil salinity or soil moisture, are extracted only at surface level, but in the study area the salinity has been inherited from the ground water and it is expected to be present at the sub surface level too, which cannot be done by multispectral remote sensing models, (3) Study of soil textural variations will increase the reliability of the result (4) Human activities are studied through LULC maps, DSSI and DSMSI model, but the incorporation of overgrazing and excessive yield estimation model may increase the quality of the work, (5) Since soil salinity, soil moisture stress and hard pans is the dominant features distributed in the surface and sub surface level, the recent advanced technology like microwave remote sensing should be employed in order to quantify the salinity regions accurately. Because of the all weather potentiality, surface penetration capability and response towards the electrical properties of the target, Microwave remote sensing can be able to provide

SED
7, 3735–3771, 2015

adequate ground for extracting the surface and sub-surface salinity and moisture than other sources such as optical and multispectral remote sensing.

Acknowledgements. We would like to express our sincere thanks to Department of Science and Technology, India, for the financial support (Grant no- DST/Inspire Fellowship/2013/1109/IF131152), without which we couldn't able to purchase the required instruments and data to carry out the research work.

We thank Climate Change and Adaptation Research, Anna University for providing the Meteorological data on time.

We also thankful to the USGS for their free distribution of long term Landsat imageries through the online data portal.

References

Abdul-Qadir, A. M. H. and Benni, T. J.: Monitoring and evaluation of soil salinity in term of spectral response using Landsat images and GIS in Mesopotamian plain/Iraq, Journal of Iraqi Desert Studies, 2, 19–32, 2010.

Adhikary, P. P., Dash, C. J., Sarangi, A., and Singh, D. K.: Hydrochemical characterization and spatial distribution of fluoride in groundwater of Delhi state, India, Indian Journal of Soil Conservation, 42, 170–173, 2014.

Allbed, A., Kumar, L., and Sinha, P.: Mapping and modelling spatial variation in soil salinity in the al hassa oasis based on remote sensing indicators and regression techniques, Remote Sens., 6, 1137–1157, 2014.

Allen, R. G., Pereira, L. S., Raes, D., and Smith, M.: Crop Evapotranspiration: Guidelines for Computing Crop Water Requirements, FAO, ISBN 92-5-104219-5, 1998.

Anbazhagan, S., Palpandian, P., Jothibasu A., Uma Maheswaran, S., Venkatesan, A., and Ramesh, V.: GIS spatial analysis for artificial recharge – a case study from drought prone area, in: Water Management – Historical Perspective and Development, edited by: Anbazhagan, S., Vasagan Publication, ISBN: 978-93-83188-01-7, available at: http://www.researchgate.net/publication/255181324_GIS_Spatial_Analysis_for_Artificial_Recharge_-_A_Case_Study_from_Drought_Prone_Area (last access: 5 June 2015), 107–133, 2013.

SED

7, 3735–3771, 2015

Bapuji, B., Sandeep, V. M., Rao, V. U. M., and Venkateswarlu, B.: Potential Evapotranspiration estimation for Indian conditions: Improving accuracy through calibration coefficients, Tech. Bull. No. 1/2012, NICRA, All India Co-ordinated Research Project on Agrometeorology, Central Research Institute for Dryland Agriculture, Hyderabad, available at: http://www.nicra-icar.in/nicrarevised/images/Books/PotentialEvapotranspirationestimation.pdf (last access: 12 March 2015), 2012.

Budihal, S. L., Ganesh Raj, K., Reddy, R. S., Natarajan, A., Paul, M. A., Bandyopadhyay, T., Thomas, J. V., Arya, A. S., and Ajai, S. K.: Assessment and Mapping of Desertification Status in Bellary District, Karnataka State using IRS Data, ISPRS, available at: http://www.isprs.org/proceedings/XXXVI/part4/budhial.pdf (last access: 15 March 2015), 36, 2005.

Census of India: Provisional population Totals – Rural and Urban Distribution, Paper 2, volume 1, series 34, office of the Registrar General & Census Commissioner, India, Data Product No.00-004-2011-Cen-Book(E), available at: http://censusindia.gov.in/2011-prov-results/paper2/prov_results_paper2_india.html (last access: 1 November 2015), 2011.

Central Ground Water Board: District Groundwater Brochure Dharmapuri District, Tamil Nadu, Technical Report Series, Ministry of Water Resources, Government of India, available at: http://cgwb.gov.in/District_Profile/TamilNadu/Dharmapuri.pdf (last access: 5 February 2015), 2009.

Chen, S. and Rao, P.: Land degradation monitoring using multi–temporal Landsat TM/ETM data in a transition zone between grassland and cropland of northeast China, Int. J. Remote Sens., 29, 2055–2073, 2008.

Dodds, P. E., Meyer,W. S., and Barton, A.: A Review of Methods to Estimate Irrigated Reference Crop Evapotranspiration across Australia, CRC for Irrigation Futures Technical Report, available at: http://www.irrigationfutures.org.au/imagesDB/news/CropEvapotranspirationCRCIFTR042005.pdf (last access: 14 March 2015), No04/05, 2005.

Geeson, N. A., Brandt, C. J., and Thornes, J. B.: Mediterranean Desertification – A Mosaic of Processes and Responses, Wiley, ISBN: 978-0-470-84448-9, available at: ftp://ftp.itc.nl/ext/noroozi_aa/Data/BOOK_DOWNLOAD/agri_soil/MediterraneanDesertification-AMosaicofProcessesandResponses.pdf (last access: 20 April 2015), 1–433, 2002.

Guo, M., Liu, Y., Wang, X. F., Matsuoka, N., and Tani, H.: Analysis of Desertification and Wood Land Distribution: A Case Study on the Balinyou Banner of Inner Mongolia, China, International Society for Photogrammetry and Remote Sensing Proceedings, http://www.isprs.

SED
7, 3735–3771, 2015

org/proceedings/2011/ISRSE-34/211104015Final00042.pdf (last access: 13 June 2015), 34, 2011.
Hanan, N. P., Prince, S. D., and Hiernaux, P. H. Y.: Spectral modeling of multi component landscapes in the Sahel, Int. J. Remote Sens., 12, 1243–1258, 1991.
Hill, J.: LADAMER: Land and Soil Degradation Assessments in Mediterranean Europe, available at: https://www.uni-trier.de/fileadmin/fb6/prof/FER/Bilder-Forschung/Ladamer/GMES-Paper_Nordwijk.pdf, (last access: 29 February 2008), 2005.
Izzo, M., Araujo, N., Aucelli, P. P. C., Maratea, A., Sánchez, A.: LAND sensitivity to desertification in the dominican republic: AN adaptation of the ESA methodology, Land Degrad. Dev., 24, 486–498, doi:10.1002/ldr.2241, 2013.
Kassas, M.: Arid and Semi-arid Lands: Problems and Prospects, Agro-Ecosystem, Elsevier Scientific Publishing Company, the Netherlands, http://kassas.org/wp-content/uploads/2013/03/026.pdf (last access: 7 April 2015), 3, 185–204, 1977.
Kundu, A. and Dutta, D.: Monitoring desertification risk through climate change and human interference using Remote sensing and GIS techniques, International Journal of Geomatics and Geosciences, 2, 21–33, 2011.
Lin, N.-F. and Tang, J.: Geological environment and causes for desertification in arid-semi-arid regions in China, Environ. Geol., 41, 806–815, 2002.
Metternicht, G. and Zinck, J. A. (Eds.): Remote Sensing of Soil Salinization: Impact on Land Management, Taylor and Francis Group, LCC, CRC Press, Boca Raton, FL, USA, ISBN 978-1-4200-6502-2, 2009.
Meyer, P., Itten, K. I., Kellenberger, T., Sandmeier, S., and Sandmeier, R.: Radiometric corrections of topographically induced effects on landsat TM data in an Alpine environment, ISPRS J. Photogramm., 48, 17–28, 1993.
Moran, M. S., Clarke, T. R., Inoue, Y., and Vidal, A.: Estimating crop water deficit using the relation between surface–air temperature and spectral vegetation index, Remote Sens. Environ., 49, 246–263, 1994.
Nagler, P.L, Glenn, E.P, Kim, H., Emmerich, W., Scott, R. L., Huxman, T. E., and Huete, A. R.: Relationship between evapotranspiration and precipitation pulses in a semi-arid rangeland estimated by moisture flux towers and MODIS vegetation indices, J. Arid Environ., 70, 443–462, 2007.

SED
7, 3735–3771, 2015

Naseri, M. Y.: Characterization of salt-affected soils for modeling sustainable land management in semi-arid environment; a case study in the Gorgan region, Northeast Iran, PhD Thesis, Ghent University, Belgium, 281–287, 1998.
Nicholson, S. E., Davenport, M. L., and Malo, A. R.: A comparison of the vegetation response to rainfall in the Sahel and East Africa using normalized difference vegetation index from NOAA AVHRR, Climatic Change, 17, 209–241, 1990.
Ramesh, K. and Vennila, S.: Fluoride contamination in drinking water in Palacode Region, Tamil Nadu, International Journal of Research in Chemistry and Environment, 2, 116–123, 2012.
Rasmussen, K., Fog, B., and Madsen, J. E.: Desertification in reverse? Observations from northern Burkina Faso, Global Environ. Chang., 11, 271–282, 2001.
Roxo, M. J., Casimiro, P., and Tiago, M. S.: What is Desertification, Desert Links project, Framework- European Union, Geografia e Planeamento Regional – Faculdade de Ciências Sociais e Humanas – Universidade Nova de Lisboa, available at: https://www.kcl.ac.uk/projects/desertlinks/downloads/deliverables/Deliverable%201.2b_en.pdf (last access: 2 February 2015), 2001.
Runnstrom, M. C.: Rangeland development of the Mu Us sandy land in semi-arid china: an analysis using landsat and NOAA remote sensing data, Land Degrad. Dev., 14, 189–202, 2003.
Sandholt, I., Rasmussen, K., and Andersen, J.: A simple interpretation of the surface temperature/vegetation index space for assessment of soil moisture status, Remote Sens. Environ., 79, 213–224, 2002.
Sendesh Kannan, K., Ramasubramanian, V., and Sathyaraj, S. R.: Identification of fluoride contaminations with the interaction of physio-chemical characteristic in groundwater of Dharmapuri District, TamilNadu, INDIA, Archives of Applied Science Research, 3, 336–351, 2011.
Shafian, S. and Maas, S. J.: Index of soil moisture using raw landsat image digital count data in Texas High Plains, Remote Sens., 7, 2352–2372, 2015.
Sharmia, S.: DESERTIFICATION – about drought, desertification and poverty in the drylands, Google Blog, available at: https://desertification.wordpress.com/2008/06/23/excessive-irrigation-promotes-desertification-google-the-new-nation/ (last access: 3 June 2015), 2008.
Shewale, M. P. and Shravan, K.: Climatological features of Drought incidences in India, Meteorological Department Report, National climate centre, Office of the additional director general of meteorology (Research), India Meteorological Department, Pune, available

SED
7, 3735–3771, 2015

at: http://www.imdpune.gov.in/research/drought/DROUGHT_CLIMATOLOGY_1.pdf (last access: 13 June 2015), 2005.
UNCCD: United Nations Convention to Combat Desertification, Geneva, Switzerland, United Nations, available at; https://www.kcl.ac.uk/projects/desertlinks/downloads/deliverables/Deliverable%201.2b_en.pdf (last access: 3 March 2015), 58 pp., 1994.
UNCCD: Zero Net Land Degradation – A Sustainable Development Goal for Rio +20, UNCCD Secretariat Recommendations for Policymakers, available at: http://www.unccd.int/Lists/SiteDocumentLibrary/Rio+20/UNCCD_PolicyBrief_ZeroNetLandDegradation.pdf, ISBN978-92-95043-62-6 (last access: 3 March 2015), ISBN 978-92-95043-62-6, 2012.
U.S. Dept. of Agriculture. Soil Conservation Service. Soil Survey Staff.: Soil Taxonomy: A Basic System of Soil Classification for Making and Interpreting Soil Surveys, U.S. Dept. of Agric. Handb. 436, U.S. Govt. Print. Off. Washington, DC, 754 pp., illus, 1975.
Vieira, R. M. S. P., Tomasella, J., Alvalá, R. C. S., Sestini, M. F., Affonso, A. G., Rodriguez, D. A., Barbosa, A. A., Cunha, A. P. M. A., Valles, G. F., Crepani, E., de Oliveira, S. B. P., de Souza, M. S. B., Calil, P. M., de Carvalho, M. A., Valeriano, D. M., Campello, F. C. B., and Santana, M. O.: Identifying areas susceptible to desertification in the Brazilian northeast, Solid Earth, 6, 347–360, doi:10.5194/se-6-347-2015, 2015.
Wessels, K. J., Prince, A. S., Carroll, M., and Malherbe, J.: Relevance of rangeland degradation in semi-arid north eastern South Africa to the non-equilibrium theory, Ecol. Appl., 17, 815–827, 2007.
Williams, D. L., Goward, S., and Arvidson, T.: Landsat: yesterday, today, and tomorrow, Photogramm. Eng. Rem. S., 72, 1171–1178, 2006.
Xunming, W., Fahu, C., and Zhibao, D.: The relative role of climatic and human factors in desertification in semi-arid China, Global Environ. Chang., 16, 48–57, 2006.

SED
7, 3735–3771, 2015

Table 1. Hypothesis combinations, computed t values with 1 % level of significance, corresponding probability (p score) and decision taken based on the tabulated values.

S.No	Hypothesis variables	p value	Degrees of Freedom	t value	Decision
1	Temperature – Salinity	0.004	$n-2$	4.645	High Significance
2	Wind Speed – Moisture stress	0.005	$n-2$	3.576	High Significance
3	Rainfall – Moisture presence	0.005	$n-2$	−3.248	High Significance

SED
7, 3735–3771, 2015

Table 2. Statistical measure of the chemical parameters at sampled locations. EC and Salinity follows positive correlation with pH in the alkaline range (> 7). The moisture content is below 35 % in all four zones of desertification. In temperature affected region the higher salinity is found at sub-surface level because of the fluoride concentration in ground water. We found the inverse relationship in human induced desertified zone i.e., the surface salinity is higher than the sub-surface and the standard deviation of surface level salinity is lesser than the sub-surface, which indicates that the human made salinity is not fluctuating at surface level because of the constant application of fertilizers more than two decades. Surface level soil moisture stress is highly observed in the wind and rainfall induced desertified regions.

Chemical Properties	Temperature induced desertified region				Human induced desertified region				Wind and Rainfall induced desertified region			
	Surface Level		Sub-surface Level		Surface Level		Sub-surface Level		Surface Level		Sub-surface Level	
	Mean	Std	Mean	Std	Mean	Std	Mean	Std	Mean	Std	Mean	Std
pH	7.90	0.9	8.10	0.40	8.80	0.28	7.74	1.10	7.00	1.49	7.46	0.72
EC ($mS\,cm^{-1}$)	3.73	1.1	4.65	0.43	5.10	0.85	4.4	1.46	2.05	1.6	3.12	0.7
Salinity (ppt)	3	1.5	4.2	0.50	4.35	0.93	3.15	1.49	1.90	1.44	3.10	0.95
Soil moisture (%)	19	1.53	30.0	1.02	20.0	1.26	32.0	1.10	15.0	1.34	31.0	1.00

SED
7, 3735–3771, 2015

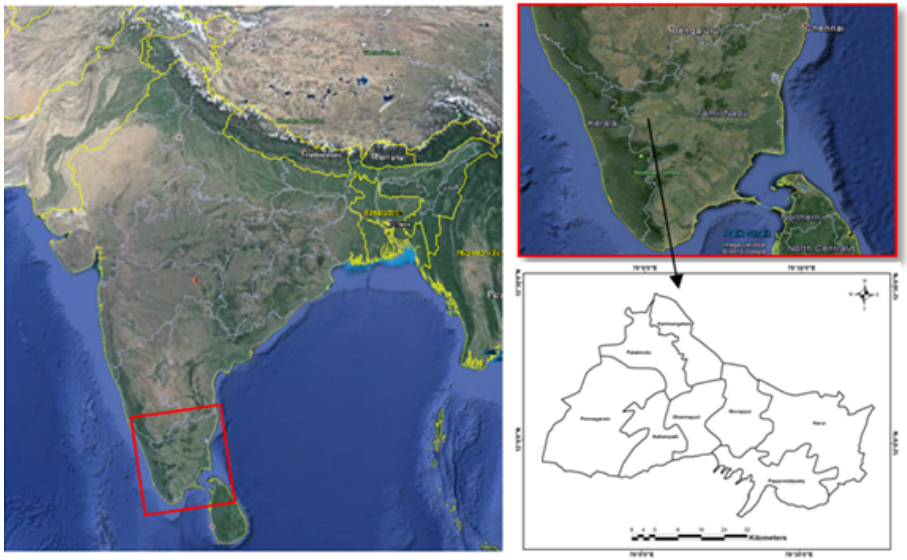

Figure 1. Study area- Dharmapuri District of Tamil Nadu, India. It is the staring example of semi-arid regions across the world where the 70 % of the population rely on dry land agriculture. The annual evapotranspiration rate exceeds the rate of rainfall because of its locality under rain-shadow region of Western Ghats. Extreme temperature prevalence, native fluoride nature and unsustainable agricultural practices have made the region to experience drought often leads to desertification.

SED
7, 3735–3771, 2015

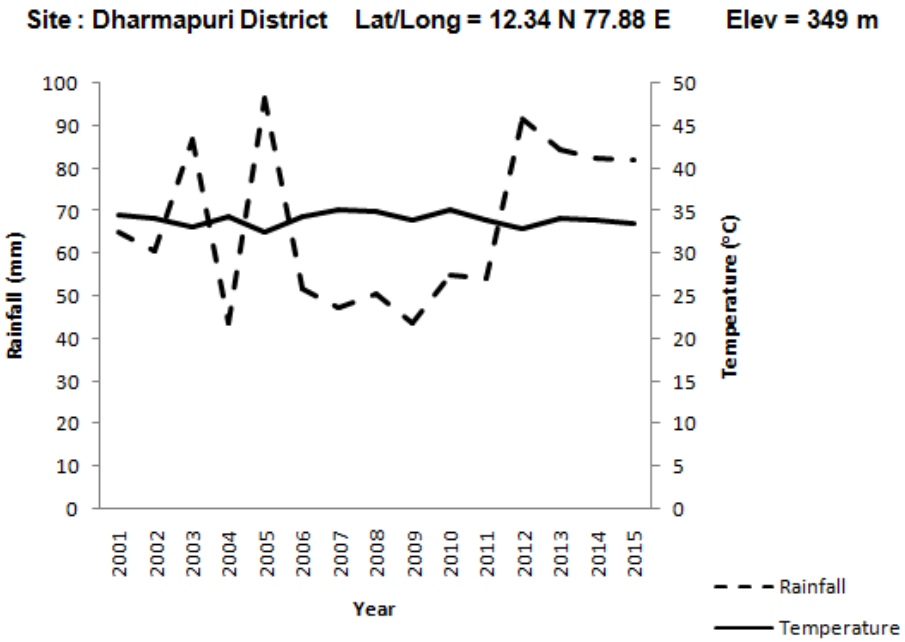

Figure 2. Climate diagram for one meteorological Station (Nallampalli) – Rainfall Vs Temperature for the crop growing period (June–October) from 2001–2015. The significant drought period was observed from 2006–2011 followed by adequate rainfall distribution (2012–2015) which is appropriate for crop production. If the degraded land (2006–2011) is not renewed or regenerated after receiving sufficient rainfall occurred from 2012–2015, then it is termed as desertification else, it is just degradation.

SED
7, 3735–3771, 2015

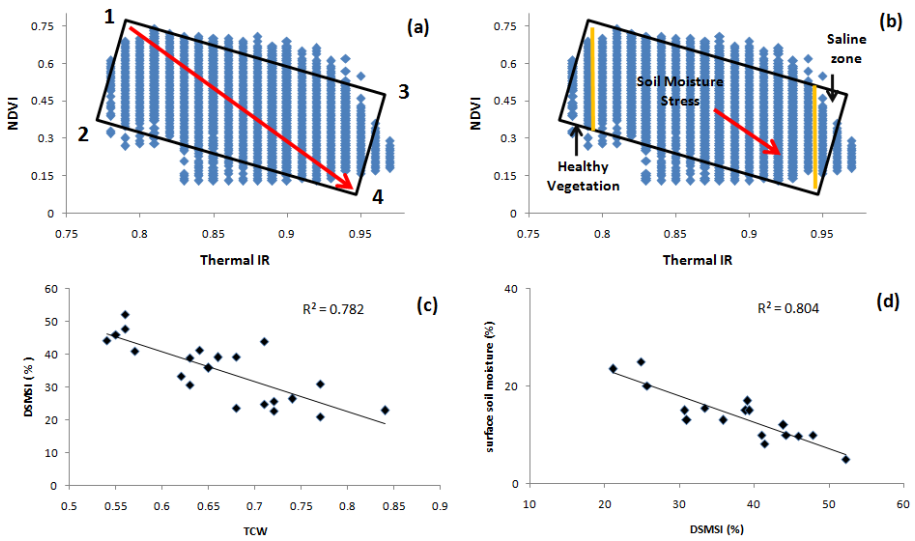

Figure 3. (a) Scatter plot – Thermal IR Vs NDVI – Diagrammatic approximation of the distribution – Diagonal from extreme wet edge 1 to extreme dry edge 4. **(b)** Three zones of scatter plot such as healthy zone with maximum NDVI and low temperature, soil moisture stress zone which keeps on increasing with increasing diagonal distance from wet edge and saline zone at the extreme portion of the rectangle where the temperature is high and NDVI is almost zero. **(c)** Linear regression between Diagonal Soil Moisture Stress Index (DSMSI) and Tasseled cap wetness index (TCW) (R^2 = 0.782) to ensure the theoretical reliability of the result. **(d)** Linear regression between DSMSI and in situ observations agrees with good accuracy (R^2 = 0.804) of the model.

SED
7, 3735–3771, 2015

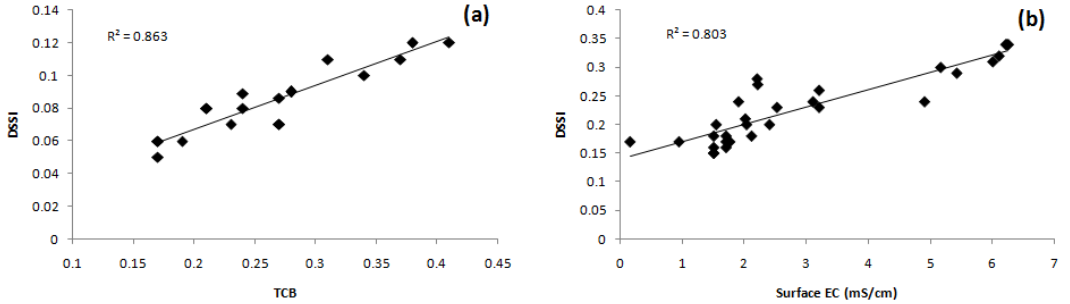

Figure 4. (a) Diagonal Soil Salinity Index (DSSI) model confirms theoretical accuracy with Tasseled cap Brightness index (TCB) (R^2 = 0.863). **(b)** Linear regression between DSSI and Surface Electrical Conductivity (EC) (R^2 = 0.803) which ensures the ground reliability of the model.

SED
7, 3735–3771, 2015

Figure 5. (a) Questionnaire survey with local farmer. **(b)** Direct in situ measurement to evaluate the chemical properties of the soil. **(c)** Highly saline affected region. **(d)** Soil moisture stress zone. **(e)** Land reclamation process hampered because of the presence of hard pans. **(f)** Soil samples collected for testing the chemical properties.

SED
7, 3735–3771, 2015

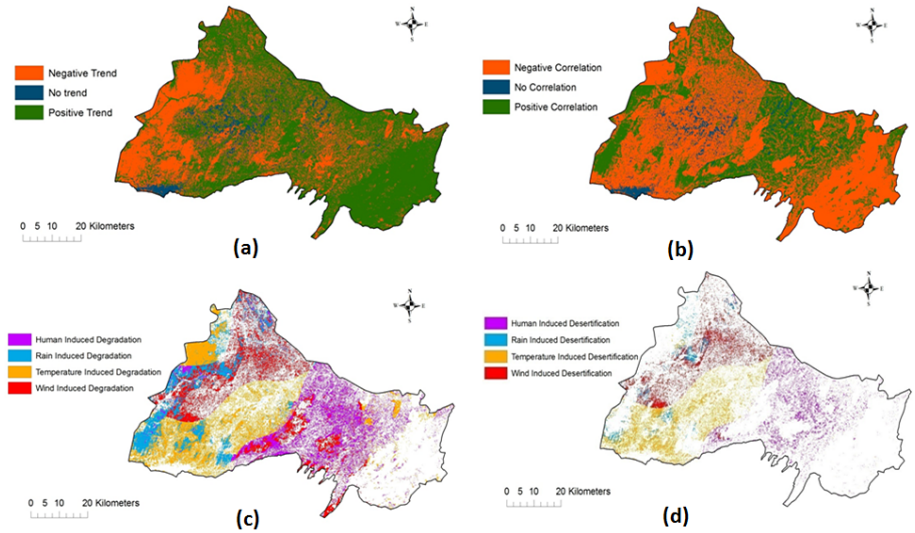

Figure 6. (a) Block wise $NDVI_{observed}$ Trend. Area of no correlation in the Fig. 6b is exactly coincided with no change area of Fig. 6a i.e this is the place of no correlation between ET_{ref} and NDVI due to the presence of stable NDVI over a period of time. **(b)** Correlation coefficient map for $ET_{ref\text{-}mean}$ and $NDVI_{predicted\ mean}$ for 12 years. Eastern and western part of the study region has been experiencing high negative correlation over a period. High positive correlation has been observed in the middle part of the region. **(c)** Block wise distribution of degraded land with respect to four crucial causative factors. **(d)** Block wise distribution of desertified land extracted from degraded zones after the assessment with short term $NDVI_{observed}$ trend (2013 and 2014). Western part of the region has got combined effect by temperature, rainfall and wind. Though the eastern part receives adequate rain and experiences moderate temperature and wind which is appropriate for vegetation production, the distribution of desertified land is higher due to anthropogenic activities.

SED
7, 3735–3771, 2015

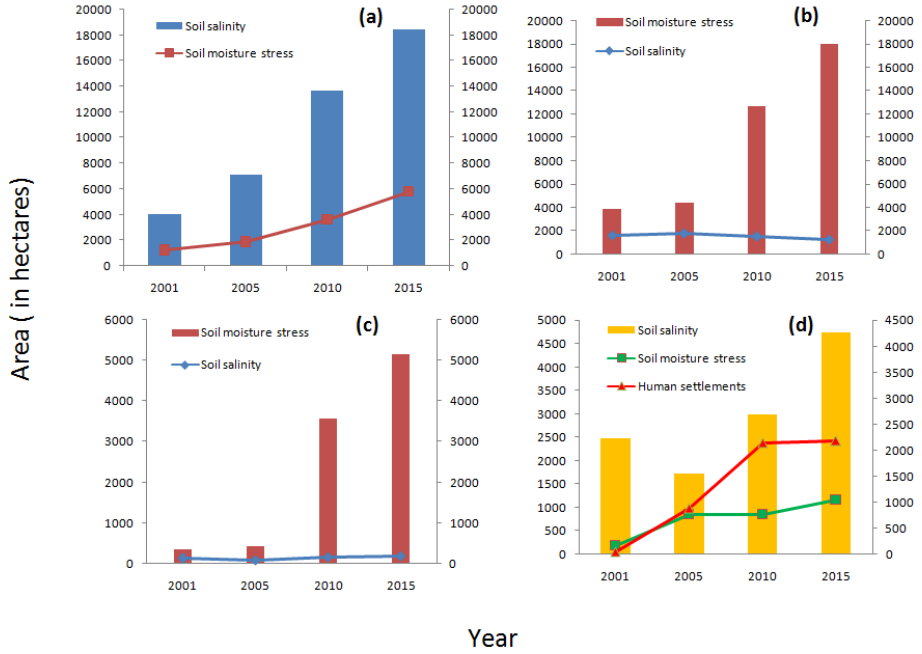

Figure 7. (a) Areal extent of soil moisture and soil salinity for temperature affected zone from 2001 to 2012 in which the growth of saline affected regions is in high proportion than the moisture affected due to native fluoride content and clayey soil origin. **(b)** Areal extent of soil moisture and salinity for wind affected zone from 2001–2012. The soil moisture stress has been accelerated in the wind affected zone than the salinity. **(c)** Areal extent of soil degradation processes in rainfall affected region. **(d)** Soil salinity, moisture stress and human occupancy are together observed in the human affected region from 2001–2014. Human settlements are elevated in a higher rate followed by man-made salinity and soil moisture stress.

SED
7, 3735–3771, 2015

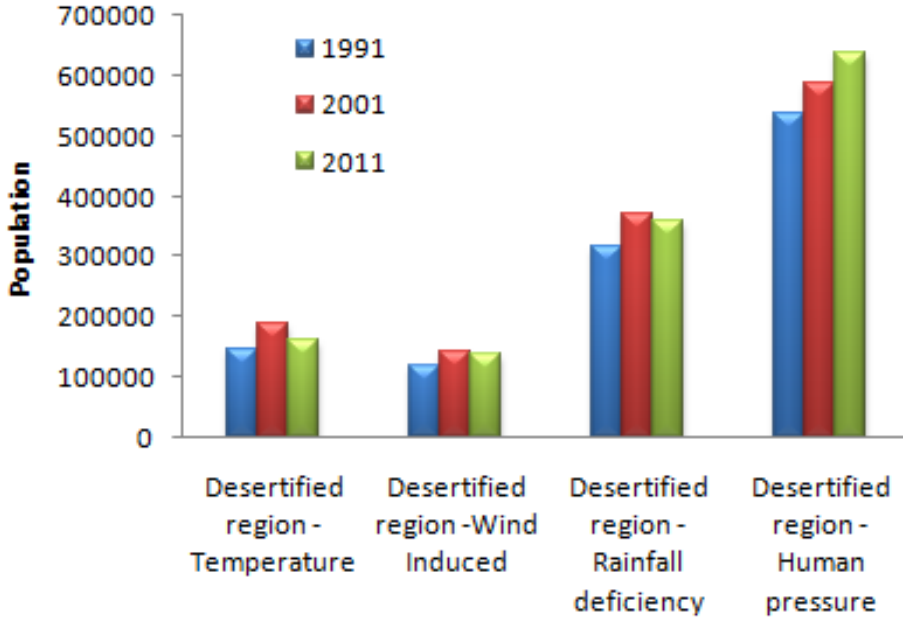

Figure 8. Population trend of four zones of desertification from 1991–2011. The population trend has been significantly increased (8 %) from 2001–2011 in the human induced desertified zone, where as in the temperature, wind and rainfall affected zone it follows decreasing trend. This is because of the migration of the inhabitants towards urbanized area in order to stabilize their economical needs during drought period.

SED
7, 3735–3771, 2015

Copyright of Solid Earth Discussions is the property of Copernicus Gesellschaft mbH and its content may not be copied or emailed to multiple sites or posted to a listserv without the copyright holder's express written permission. However, users may print, download, or email articles for individual use.